



## Multimodal ionic liquid-based chromatographic supports for an effective RNA purification

Rita Carapito<sup>a</sup>, Sandra C. Bernardo<sup>a</sup>, Matheus M. Pereira<sup>b</sup>, Márcia C. Neves<sup>c</sup>, Mara G. Freire<sup>c,\*</sup>, Fani Sousa<sup>a,\*</sup>

<sup>a</sup> CICS-UBI – Health Sciences Research Centre, University of Beira Interior, Av. Infante D. Henrique, 6200-506 Covilhã, Portugal

<sup>b</sup> University of Coimbra, CIEPQPF, Department of Chemical Engineering, Rua Sílvio Lima, Pólo II – Pinhal de Marrocos, 3030-790 Coimbra, Portugal

<sup>c</sup> CICECO – Aveiro Institute of Materials, Chemistry Department, University of Aveiro, 3810-193 Aveiro, Portugal

### ARTICLE INFO

#### Keywords:

Nucleic acids  
Ionic liquid  
Ionic liquid-based support  
Multimodal ligand  
Purification

### ABSTRACT

Nucleic acids have been considered interesting molecules to be used as biopharmaceuticals for the treatment of various diseases, in gene therapy strategies. In particular, RNA arises as the most promising approach because it does not require access to the nucleus of cells to exert its function; however, it is quite challenging due to its labile nature. To increase the possibility of translating RNA-based technology to clinical protocols, the bio-manufacturing of RNAs has been intensively exploited in the last few years. However, the standard RNA purification processes remain time-consuming and present limitations regarding recovery yield and purity. This work describes the functionalization of chromatographic silica-based supports with four ionic liquids (ILs) composed of functional moieties that can promote distinct interactions with nucleic acids. After an initial screening to evaluate the binding and elution behavior of nucleic acids in the IL-based supports, SSI[C<sub>3</sub>C<sub>3</sub>NH<sub>2</sub>Im]Cl has shown to be the most promising for further purification assays. This support was studied for the RNA purification from different samples (clarified or more complex) and has shown to be highly effective, for all the conditions studied. Generally, it is here presented a new method for RNA isolation in a single step, using an IL-based chromatographic support, able to eliminate the usage of hazardous compounds often included in standard RNA extraction protocols.

### 1. Introduction

Therapies based on nucleic acids are emerging as personalized medicine, with great potential for treating numerous diseases, especially those caused by gene defects. Gene therapy or DNA/RNA vaccination is based on the administration of nucleic acids as biopharmaceuticals aiming to correct genetic defects or induce an immune response [1,2]. In recent years, RNA gained more relevance due to the identification of an increasing number of biological roles, including regulatory and enzymatic functions. RNA presents high potential to be explored as a biomarker for the diagnosis of certain diseases or as a pharmaceutical agent, regulating the levels of numerous proteins involved in different cellular processes.

In order to study and understand RNA functions and perform biochemical, biophysical, and genetic studies, sample preparation is required, and most techniques are still in development [3]. The

available methods are mostly adequate for molecular biology procedures, but if it is intended the preparation of RNAs for therapeutic purposes, other challenges must be overcome since methods must be improved in accordance with the product requirements [2,4–6]. RNAs have been obtained through different procedures, such as *in vitro* synthesis, chemical synthesis, and recombinant production [7]. FDA has already approved the first two methods, however, recombinant production is more capable of retaining the structure, function, and safety properties of natural RNAs and also offers more perspectives for large-scale production [3,5]. Nevertheless, this production method makes it crucial to isolate and purify the target nucleic acids from all cellular impurities, like cell debris, endotoxins, proteins, and host DNA or RNA. In this sense, chromatography arises as the method of choice for the purification of biomolecules. Chromatography allows isolating different high value products based on the physical–chemical differences that can be exploited on the interaction with chromatographic ligands. The most

\* Corresponding authors.

E-mail addresses: [rita.carapito@fcsaude.ubi.pt](mailto:rita.carapito@fcsaude.ubi.pt) (R. Carapito), [sandra.bernardo@ubi.pt](mailto:sandra.bernardo@ubi.pt) (S.C. Bernardo), [matheus@eq.uc.pt](mailto:matheus@eq.uc.pt) (M.M. Pereira), [mcneves@ua.pt](mailto:mcneves@ua.pt) (M.C. Neves), [maragfreire@ua.pt](mailto:maragfreire@ua.pt) (M.G. Freire), [fani.sousa@fcsaude.ubi.pt](mailto:fani.sousa@fcsaude.ubi.pt) (F. Sousa).

<https://doi.org/10.1016/j.seppur.2023.123676>

Received 31 January 2023; Received in revised form 20 March 2023; Accepted 21 March 2023

Available online 24 March 2023

1383-5866/© 2023 The Authors. Published by Elsevier B.V. This is an open access article under the CC BY-NC-ND license (<http://creativecommons.org/licenses/by-nc-nd/4.0/>).

used chromatographic methods are ion-exchange, ion-pairing, reversed-phase and gel filtration. However, these methods are time-consuming and the general performance still present limitations regarding the recovery yield and product purity [5,8–10]. Therefore, new chromatographic supports with better selectivity, robustness, and reproducibility are in great demand. In this field, Ionic Liquids (ILs) arise as promising compounds to be explored as alternative chromatographic ligands.

ILs are essentially organic salts that, in contrast with common electrolytes, are liquid at lower temperatures due to their high charge distribution and low lattice energy. By being constituted of ions, ILs have an enormous versatility of chemical structures, being thus considered task-specific compounds [11–13]. If properly designed, ILs present some outstanding features, including low volatility, non-flammability, adequate viscosity, high solvation ability, and excellent chemical, thermal and electrochemical stabilities [11,12,14]. The ILs usage has been extended to many fields of industry like chemistry, electrochemistry, nanotechnology, medicine, material production, power engineering, biotechnology, among others [13,15]. In the last two decades, ILs have been used in liquid chromatography in three distinct ways: as additives of the mobile phase, as the stationary phase itself, or as ligands of the stationary phase [16–18]. Our research group recently developed a preparative chromatographic process for the effective purification of nucleic acids using an IL-functionalized support [4]. Nonetheless, these types of supports still need to be improved regarding their selectivity and performance at recognizing specific molecules in preparative chromatography [19,20].

This work describes the synthesis of novel chromatographic supports (spherical silica - SSI) modified with four different ILs: 1-methylimidazole (SSi[C<sub>3</sub>C<sub>1</sub>Im]Cl), N,N-dimethylbutylamine (SSi[N<sub>3114</sub>]Cl), N,N-dimethylethylenediamine (SSi[N<sub>3112NH<sub>2</sub></sub>]Cl), and 1-(3-aminopropyl)imidazole (SSi[C<sub>3</sub>C<sub>3NH<sub>2</sub></sub>Im]Cl). The respective molecular structures are provided in Fig. 1. The SSi[C<sub>3</sub>C<sub>1</sub>Im]Cl presents the same IL ligand previously studied by our research group [4]; SSi[C<sub>3</sub>C<sub>3NH<sub>2</sub></sub>Im]Cl is similar but contains an amine group that is intended to contribute to a more effective or specific interaction with the nucleic acids. SSi[N<sub>3114</sub>]Cl and SSi[N<sub>3112NH<sub>2</sub></sub>]Cl present alkyl chain lengths of different size, with SSi[N<sub>3112NH<sub>2</sub></sub>]Cl also presenting an amine group. Among these four different supports, which vary in functional groups, it was expected to select the most interesting for RNA purification strategies. These silica-based-ILs (SILs) were further evaluated regarding the RNA binding and elution profiles, in order to explore their multimodal capability. After

this initial screening, further chromatographic assays were performed in AKTA Avant® using the best-performing support for the purification of RNA.

## 2. Materials and methods

### 2.1. Materials

Silica gel spherical (75–200 μm) was from Supelco and hydrochloric acid (purity 37%) from Sigma-Aldrich (St. Louis, Missouri, USA). Toluene (purity 99.98%) and ethanol (purity 99.99%) were acquired from Fisher Scientific (Massachusetts, USA), methanol (purity < 98%) from Fisher Chemical (Waltham, USA), and (3-chloropropyl)trimethoxysilane (purity 98%) and 1-methylimidazole (purity 99%) from Acros Organics (Geel, Belgium). N,N-dimethylbutylamine (purity 99%) and 1-(3-Aminopropyl)imidazole (purity 98%) from Aldrich (St. Louis, Missouri, USA), and N,N-Dimethylethylenediamine (purity 97%) was acquired from Alfa Aesar (Massachusetts, USA).

Tryptone and yeast extract were both from Bioakar (Beauvais, France), glycerol from Himedia, dipotassium hydrogen phosphate (K<sub>2</sub>HPO<sub>4</sub>) from Panreac (Barcelona, Spain), potassium dihydrogen phosphate (KH<sub>2</sub>PO<sub>4</sub>) from Sigma-Aldrich (St. Louis, Missouri, USA), “Luria-Broth Agar” from Pronalab (Mérida, Yucatán, Mexico) and kanamycin from Thermo Fisher Scientific Inc. (Waltham, USA). Guanidine thiocyanate, N-Lauroylsarcosine sodium salt, sodium citrate and isoamyl alcohol were from Sigma-Aldrich (St. Louis, Missouri, USA), isopropanol was from Thermo Fisher Scientific Inc. (Waltham, USA), and β-mercaptoethanol from Merck (Whitehouse Station, USA). All solutions were prepared with Milli-Q water treated with 0.01% of diethyl pyrocarbonate (DEPC) from Sigma-Aldrich (St. Louis, Missouri, USA). Molecular weight marker and Green-Safe were purchased from Grisp (Porto, Portugal). The Cell Proliferation Kit I (MTT) was from Merck (Darmstadt, Germany). “Dulbecco’s Modified Eagle’s Medium/Nutrient Mixture F-12” (DMEM-F12) was from Sigma-Aldrich (St. Louis, Missouri, USA), fetal bovine serum (FBS) was from Gibco, Life Technologies (USA), and penicillin–streptomycin was from Grisp (Porto, Portugal).

### 2.2. Synthesis and characterization of IL-based supports

#### 2.2.1. Ligands immobilization

For the functionalization of the silica support, it was first performed

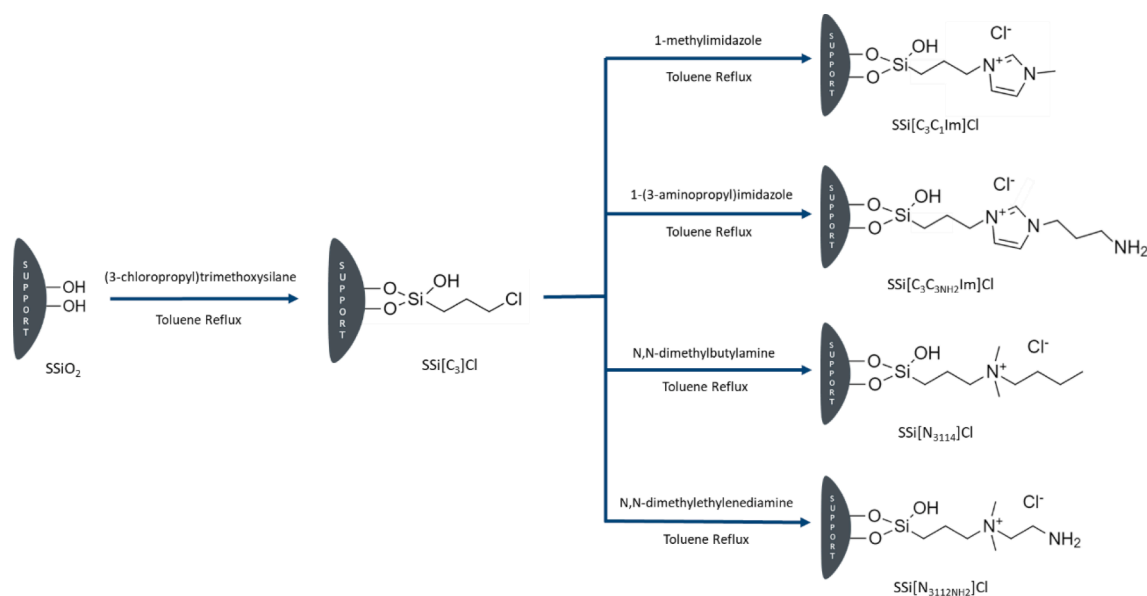


**Fig. 1.** Schematic representation of the chemical reactions performed for the functionalization of the silica supports with ILs, and corresponding molecular structures.

the activation of spherical silica gel (5 g) with hydrochloric acid (HCl) 37 % for 24 h. After this, the activated silica was washed with large volumes of distilled water, until pH reached the pH of the distilled water (approximately 7), and then dried at 100 °C in an incubator. In a second step, 5 g of activated silica were added to 60 mL of toluene (solvent of the reaction) and 5 mL of (3-chloropropyl) trimethoxysilane. The suspension was refluxed at 95 °C, and 500 rpm for 24 h. After this, the intermediate material (SSi[C<sub>3</sub>]Cl) was filtered and washed sequentially with 100 mL of toluene, 200 mL of ethanol/H<sub>2</sub>O (1:1), 500 mL of H<sub>2</sub>O and 100 mL of methanol and dried at 60 °C. Then, 5 g of SSi[C<sub>3</sub>]Cl were added to 60 mL of toluene and a certain volume (adapted from Qiu et al. [21]) of the reacted compound to originate the cation of interest. For example, adding 1-methylimidazole in toluene reflux to the intermediate support SSi[C<sub>3</sub>]Cl, will result in the SSi[C<sub>3</sub>C<sub>1</sub>Im]Cl. The strategy was similar for all the synthesized supports, as represented in Fig. 1. The mixture was left to react for 24 h, at 110 °C and 500 rpm. The resultant materials were finally filtered and washed sequentially with 100 mL of toluene, 350 mL of methanol, 300 mL of H<sub>2</sub>O and 150 mL of methanol, and then dried at 60 °C.

### 2.2.2. Support characterization

The prepared materials (four SILs and the intermediate support) were characterized by elemental analysis, solid-State <sup>13</sup>C nuclear magnetic resonance spectroscopy (CPMAS-NMR) and Point Zero Charge (PZC). The content (weight percentage) of carbon, hydrogen and nitrogen in the materials was determined by elemental analysis, using the equipment Truspec 630–200-200, whereas the sample was burned at 1075 °C. For solid state <sup>13</sup>C NMR, each material was analyzed with the equipment Bruker Avance III 400 MHz (DSX model) using 4 mm BL cross-polarization magic angle spinning (CPMAS) VTN probes at 100.6 MHz, at room temperature. In order to determine the point where the zeta potential is zero, a residual amount of support was resuspended in water and then the zeta potential was measured at the different pH values.

### 2.3. Nucleic acid production

Production of nucleic acids was performed in *Escherichia coli* DH5α (*E. coli*) previously transformed with the plasmid pBHSR1-RM containing the sequence of human pre-miRNA29b, or in non-transformed strains, when the host biomolecules were required. *E. coli* was cultured in a plate with solid medium “Luria-Broth Agar” (LB-Agar) supplemented with 50 µg/mL of kanamycin, overnight, at 37 °C. Then, cultures were performed in “Terrific Broth” medium (TB): 12 g/L of tryptone, 24 g/L of yeast extract, 5.5x10<sup>-5</sup> M of glycerol, 0.017 M of KH<sub>2</sub>PO<sub>4</sub> and 0.072 M of K<sub>2</sub>HPO<sub>4</sub>. Pre-culture medium was inoculated with *E. coli* from the plaque and incubated at 37 °C, with 250 rpm of shaking. Optical Density (OD) was measured at 600 nm, using a spectrophotometer Pharmacia Biotech Ultraspec 3000 UV/Visible (Cambridge, England), until OD reached 2.6. The culture was then inoculated from the pre-culture, to initiate at an OD of 0.2. The growth was kept for 8 h and lastly centrifuged at 3900 g, 4 °C, for 10 min, and cell pellets were stored at –20 °C. Since the *E. coli* culture was carried out for 8 h (late exponential phase), the RNAs that are found in higher quantity are mainly smaller RNAs such as 6S RNA, tRNA, and other non-coding RNAs that range from 50 to 300 bases in size. If we intend to have ribosomal RNA, we would need to perform an *E. coli* culture of about 3 h corresponding to the early exponential phase [22].

### 2.4. RNA extraction

RNA extraction was performed by the method of acid guanidinium thiocyanate-phenol-chloroform as described previously by our research group [4,22]. Firstly, the *E. coli* pellets were resuspended with 5 mL of D Solution (4 M guanidinium thiocyanate, 0.025 M sodium citrate pH 7, 0.5 % sodium N-lauroylsarcosinate and 0.1 M β-mercaptoethanol) and incubated in ice for 10 min. After this, 0.5 mL of 2 M sodium acetate pH

4 and 5 mL of phenol were added to the suspensions, being carefully homogenized at each step. Then, 1 mL of a mixture of chloroform/isomyl alcohol (49:1) was added followed by vigorous shaking and incubation in ice, for 15 min. The suspensions were centrifuged at 10,000 g for 20 min at 4 °C. Two aqueous phases were formed, being the upper phase enriched in RNA, which must be very carefully transferred to new tubes, avoiding DNA contamination (from the bottom phase). To these new tubes, 5 mL of isopropanol were added to precipitate RNA, which was recovered by centrifugation at 10,000 g for 20 min at 4 °C. RNA pellets were dissolved in 1.5 mL of D Solution, and then 1.5 mL of isopropanol, followed by centrifugation at 10,000 g for 10 min at 4 °C. The resultant pellets were resuspended in 2.5 mL of 75 % ethanol in DEPC water, incubating the samples at room temperature for 10–15 min, followed by a centrifugation at 10,000 g for 5 min at 4 °C. The pellet was then dried for 5–10 min at room temperature. Finally, RNA pellets were dissolved in 1 mL of DEPC treated water and incubated at room temperature for 10–15 min. The concentration of RNA was measured in the Nano Photometer (IMPLEN, United Kingdom) and integrity of the samples was verified by 1% agarose gel electrophoresis, being the samples stored at –80 °C.

### 2.5. Total nucleic acids extraction

For the extraction of all nucleic acids from *E. coli* cells, the protocol was initiated with chemical lysis as described previously by our research group [4]. Pellets were resuspended in 5 mL of D Solution (same composition as above), allowing the disruption of cells. Then, the lysis tubes were incubated in ice for 10 min, following a centrifugation at 16,000 g for 30 min at 4 °C. The supernatant was recovered and mixed with 5 mL of isopropanol. The tubes were incubated in ice for 30 min and then centrifuged at 16,000 g for 20 min at 4 °C. After discarding the supernatant, 2.5 mL of 75 % ethanol-DEPC were added to each tube followed by room temperature incubation for 10 min. A centrifugation at 16,000 g for 5 min at 4 °C was performed, the supernatant was discarded, and the pellets were air-dried for 10 min. Pellets were suspended in 2 mL of DEPC treated water and incubated in a 60 °C water bath for 10 min, and finally centrifuged at 16,000 g for 30 min at 4 °C, being the supernatant recovered. The concentration and integrity of the samples was assessed as described in the previous topic.

### 2.6. Screening of RNA binding/elution profiles with different supports

For the screening of RNA behavior in terms of binding and elution to the different supports, each one of the synthesized materials was packed in a column. For this, each support was added to the column until it reached 2 cm of height. All the supports were washed with large volumes of water and then closed with a filter, keeping the support always hydrated. To determine the best binding and elution conditions, different gradients were studied, to mainly exploit electrostatic or hydrophobic interactions. To mainly favor electrostatic interactions, the columns were first equilibrated with 10 mL of 10 mM K<sub>2</sub>HPO<sub>4</sub>/KH<sub>2</sub>PO<sub>4</sub> pH 8, allowing it to empty by gravity flow, followed by injection of approximately 30 µg of low molecular weight RNA. Binding step was favored by applying 10 mL of the same buffer (10 mM K<sub>2</sub>HPO<sub>4</sub>/KH<sub>2</sub>PO<sub>4</sub> pH 8), collecting fractions of 1 mL for further analysis. The elution was carried out by adding 10 mL of 1.5 M NaCl in 10 mM K<sub>2</sub>HPO<sub>4</sub>/KH<sub>2</sub>PO<sub>4</sub> pH 8, also collecting the fractions of 1 mL for further evaluation. For the second strategy, intended to mainly promote hydrophobic interactions, the exactly same protocol was performed, however 1.5 M (NH<sub>4</sub>)<sub>2</sub>SO<sub>4</sub> in 10 mM K<sub>2</sub>HPO<sub>4</sub>/KH<sub>2</sub>PO<sub>4</sub> pH 8 was used as binding buffer and 10 mM K<sub>2</sub>HPO<sub>4</sub>/KH<sub>2</sub>PO<sub>4</sub> pH 8 as elution buffer. At the end of each assay, columns were washed with DEPC treated water, and the absorbance of all the fractions was measured in the Nano Photometer (IMPLEN, United Kingdom).

## 2.7. Selectivity for nucleic acids (RNA vs DNA)

The separation of different nucleic acids (DNA and RNA) was studied for the support that showed better results in the screening experiments. These chromatographic assays were performed in the equipment AKTA Avant® with the software UNICORNTM 6.3 (GE Healthcare Biosciences Uppsala, Sweden) aiming at achieving the best process control and performance. The SSi[C<sub>3</sub>C<sub>3</sub>NH<sub>2</sub>Im]Cl support was packed in a HiScale 16 column (Cytiva, Sweden) with 16 mm diameter × 10 mm of height. Before each chromatographic assay, the column was equilibrated with a 10 mM K<sub>2</sub>HPO<sub>4</sub>/KH<sub>2</sub>PO<sub>4</sub> (pH 8) solution previously filtered and sonicated, using a flow rate of 1 mL/min. After equilibration, RNA or lysate samples were independently injected in a 100 µL loop. Completed the binding step, it was applied a stepwise gradient of increasing salt concentration up to 1.5 M of NaCl in 10 mM K<sub>2</sub>HPO<sub>4</sub>/KH<sub>2</sub>PO<sub>4</sub> (pH 8), in order to analyze different retention patterns and eventual species separation. A final step with higher salt concentration was performed, whenever it was needed, to guarantee the total elution of the sample. All experiments were performed at room temperature. Absorbance of eluted species was continuously monitored at 260 nm. The fractions of the elution peaks were recovered and further desalted and concentrated with concentrators Vivaspin 10000 Da (Vivascience) until reaching 100 µL, being lastly analyzed by agarose gel electrophoresis. To guarantee the reproducibility between experiments and maintain the performance of these supports, it is imperative to establish an effective regeneration protocol, that allows the elution of any species strongly retained. For that, a solution of 0.2 M of sodium hydroxide (NaOH) was added to the support in order to remove any residues of sample, followed by a solution of 0.5 M of HCl for the replacement of the counterion (Cl<sup>-</sup>) in the matrix. After every regeneration protocol, the supports were washed with large volumes of DEPC treated water.

## 2.8. Molecular docking

The intermolecular interactions between SSi[C<sub>3</sub>C<sub>3</sub>NH<sub>2</sub>Im]Cl and DNA/RNA were analyzed using molecular docking. The computational analysis was performed using the methodology applied by Nunes and co-workers [23], with protocol modifications to nucleic acids analysis. The bind score of DNA/RNA with the ligand (IL cation from SSi[C<sub>3</sub>C<sub>3</sub>NH<sub>2</sub>Im]Cl material) was calculated using the AutoDock Vina 1.1.2 program [24]. The chemical structure of ligand was created using Discovery Studio v21 (Accelrys, San Diego, CA, USA) and Chem3D-MM2 protocol was used to minimize the energy of the molecule. Macromolecular crystal structures were obtained from the PDB database (DNA: 1AOI and RNA: 1KXK), and used to prepare the receptor input files by removing protein, water and ligand molecules, merging nonpolar hydrogen atoms, adding partial charges, and adding atom types. Then, ligand and receptors docking input files were converted into.pdbqt files using AutoDockTools (ADT) [25]. The coordinates at the center of DNA grid box were 6.799 × 92.705 × -4.085 and RNA grid box were -24.215 × 47.786 × 141.754 (x-, y-, and z-axes, respectively). The grid dimension for DNA was 60 Å × 70 Å × 50 Å and for RNA was 60 Å × 60 Å × 60. The binding model with the lowest docking score for each receptor was obtained using the following configuration: *exhaustiveness* = 100, *num\_modes* = 10 and *seed* = 100.

## 2.9. Circular Dichroism (CD) spectroscopy

Circular Dichroism (CD) experiments were performed in a Jasco J-815 spectropolarimeter (Jasco, Easton, MD, USA), using a Peltier-type temperature control system, to verify the nucleic acids structural stability. CD spectra were acquired at a constant temperature of 20 °C using a scanning speed of 50 nm/min, with a response time of 1 s over wavelengths ranging from 200 to 320 nm. The recording bandwidth was of 1 nm with a step size of 1 nm using a quartz cell with an optical path length of 1 mm. Three scans were recorded per spectrum to improve the

signal-to-noise ratio and the spectra were smoothed by using the noise-reducing option in the operating software.

## 2.10. Eukaryotic cell culture and cytotoxicity assay (MTT)

Normal human dermal fibroblasts (hFIB) were used for the cytotoxicity evaluation. Cells were cultured in DMEM-F12 medium supplemented with 10 % FBS heat inactivated and 1 % penicillin–streptomycin. The cytotoxicity effect of the different supports was evaluated using the Cell Proliferation Kit I (MTT) assay. To this end, hFIB cells at passages 10–20 were seeded at a density of 1 × 10<sup>4</sup> cells per well in a 96-well plate and 24 h after, the cell culture medium was replaced by new medium, and the different supports, in different quantities, namely 25 µg, 50 µg and 100 µg, were placed in contact to the cells. MTT assay was performed at 24 and 48 h. The medium was replaced by a mixture of 100 µL of medium and 10 µL of MTT reagent, and cells were incubated during 4 h at 37 °C in a humidified atmosphere containing 5 % CO<sub>2</sub>. Following incubation, the medium was removed, and 100 µL of dimethyl sulfoxide (DMSO) were added to each well and the plate was placed in agitation for about 15 min for crystals solubilization. The absorbance measurements were performed in a microplate reader at 570 nm. All experiments were repeated three times. For cytotoxicity positive control, the cells were treated with 70 % ethanol. All cytotoxicity experiments were repeated three times using independent culture preparations. The data are expressed as mean ± standard error. Quantitative data were statistically analyzed by One-Way Analysis of Variance (ANOVA), followed by pair-wise comparisons using Dunnett's test. “\*” indicate significant difference versus untreated cells.

## 3. Results and discussion

### 3.1. Synthesis and characterization of SILs

All SILs were prepared by a two-step reaction process, summarized in Fig. 1, and then were characterized by elemental analysis, solid-State <sup>13</sup>C nuclear magnetic resonance (CPMAS-NMR) spectroscopy, and Point Zero Charge (PZC). Elemental analysis was carried out to determine the carbon, hydrogen, and nitrogen content of the prepared SILs and the intermediate material, whose results are provided in Table 1. SSi[C<sub>3</sub>]Cl does not present nitrogen, being in accordance with the expected, since this was just the intermediate material of the two-step reaction. This result also supports the absence of IL organic moieties in this material. Contrarily, it is confirmed the presence of the three analyzed elements, and particularly the nitrogen content, in all the synthesized SILs, proving that the studied ILs were efficiently immobilized on the silica surface. By considering the chemical structure of each ligand, the stoichiometry of the reaction with a yield of 100% and their respective molar mass, it was calculated the percentage of theoretical content (%TC) and the adjusted percentage without considering the silica content (%CS) for these supports. By the determined ratio of %CS/%TC presented in Table 1, it is clear that all four synthesized SILs were, in fact, efficiently functionalized onto the silica support as the values of this ratio regarding the nitrogen element are very close to 1 (ranging from 0.92 to 0.97). Additionally, the ligand density was determined, in which reproducibility in the functionalization process is seen since the value obtained with SSi[C<sub>3</sub>C<sub>1</sub>Im]Cl is in accordance to previous works [4]. Moreover, SSi[C<sub>3</sub>C<sub>1</sub>Im]Cl has shown to be more efficiently functionalized, followed by SSi[N<sub>3112</sub>NH<sub>2</sub>]Cl, SSi[C<sub>3</sub>C<sub>3</sub>NH<sub>2</sub>Im]Cl and SSi[N<sub>3114</sub>]Cl.

The successful preparation of SILs was additionally confirmed through solid-state <sup>13</sup>C Nuclear magnetic resonance (CPMAS-NMR). The results obtained are represented in Fig. 2, showing the chemical structures of the intermediate SSi[C<sub>3</sub>]Cl and the modified SILs. The corresponding carbons are designated for each respective chemical shift in the spectra (based at the estimation given by ChemDraw Software, licensed to the University of Aveiro by PerkinElmer Download Center). Concerning the SSi[C<sub>3</sub>]Cl spectrum, three peaks at 9, 27 and 47 ppm are

Table 1

Elemental analysis and ligand density results for each material. Comparison between real sample (%CS) and theoretical percentages (%TC) is provided.

| Support   | Element | Real content (weight fraction %) <sup>a</sup> | Content in Sample (%CS) | Theoretical Content (%TC) | %CS/%TC | Ligand Density (mmol of immobilized ligand per g of matrix) <sup>b</sup> |
|---|---------|---|-------------------------|---------------------------|---------|--|
| SSi[C <sub>3</sub> ]Cl                                  | C       | 4.637   | 76.886                  | 83.721                    | 0.918   | –  |
|   | H       | 1.394   | 23.114                  | 16.279                    | 1.420   | –  |
|   | N       | –   | –                       | –                         | –       | –  |
| SSi[C <sub>3</sub> C <sub>1</sub> Im]Cl                 | C       | 6.86  | 63.636                  | 67.742                    | 0.939   | 0.846  |
|   | H       | 1.55  | 14.378                  | 9.677                     | 1.486   | –  |
|   | N       | 2.37  | 21.985                  | 22.581                    | 0.974   | –  |
| SSi[C <sub>3</sub> C <sub>3</sub> NH <sub>2</sub> Im]Cl | C       | 8.189   | 64.249                  | 64.671                    | 0.993   | 0.698  |
|   | H       | 1.623   | 12.734                  | 10.180                    | 1.251   | –  |
|   | N       | 2.934   | 23.017                  | 25.150                    | 0.915   | –  |
| SSi[N <sub>3114</sub> ]Cl                               | C       | 5.64  | 73.822                  | 75.524                    | 0.977   | 0.507  |
|   | H       | 1.29  | 16.885                  | 14.685                    | 1.150   | –  |
|   | N       | 0.71  | 9.293                   | 9.790                     | 0.949   | –  |
| SSi[N <sub>3112</sub> NH <sub>2</sub> ]Cl               | C       | 6.121   | 62.483                  | 63.636                    | 0.982   | 0.700  |
|   | H       | 1.712   | 17.477                  | 15.152                    | 1.154   | –  |
|   | N       | 1.963   | 20.040                  | 21.212                    | 0.945   | –  |

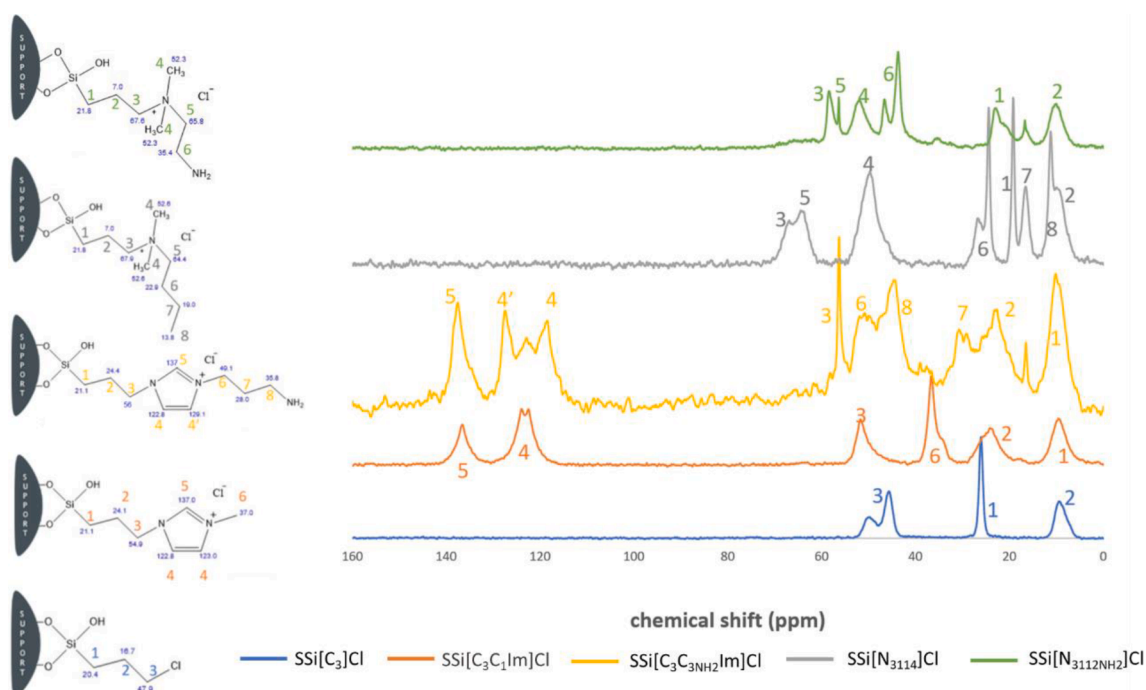
<sup>a</sup> Results obtained from elemental analysis.<sup>b</sup> Determined by  $Q = (\% \text{ weight fraction of Nitrogen}) / (1.4 \times \text{Number of nitrogen atoms})$ .

Fig. 2. CPMAS-NMR spectra of SSi[C<sub>3</sub>]Cl (blue) and the prepared SILs: SSi[C<sub>3</sub>C<sub>1</sub>Im]Cl (orange); SSi[C<sub>3</sub>C<sub>3</sub>NH<sub>2</sub>Im]Cl (yellow); SSi[N<sub>3114</sub>]Cl (grey); SSi[N<sub>3112</sub>NH<sub>2</sub>]Cl (green). It is presented the chemical structure of these compounds and the respective <sup>13</sup>C NMR estimations given by the ChemDraw Software, in which the corresponding carbons are designated for each respective chemical shift in the spectra. (For interpretation of the references to colour in this figure legend, the reader is referred to the web version of this article.)

assigned to the three carbons of the propyl alkyl chain. The spectrum of SSi[C<sub>3</sub>C<sub>1</sub>Im]Cl shows the carbon peaks assigned to the imidazolium ring at 123 and 137 ppm (C4 and C5), of the methyl chain at 37 ppm (C6), and of the propyl chain at 10, 24 and 52 ppm (C1-C3). It is possible to compare SSi[C<sub>3</sub>C<sub>1</sub>Im]Cl and SSi[C<sub>3</sub>C<sub>3</sub>NH<sub>2</sub>Im]Cl spectra, since they present the characteristic carbon peaks of the imidazolium ring (C4 and C5); however, the SSi[C<sub>3</sub>C<sub>3</sub>NH<sub>2</sub>Im]Cl spectrum differs significantly from 20 to 50 ppm by the presence of additional peaks regarding the introduction of the propylamine group (C6-C8). The spectrum of SSi[N<sub>3114</sub>]Cl shows the peaks assigned to the carbons of the propyl chain (C1-C3) at around 9, 20 and 66 ppm, the carbon of the methyl chains (C4) at 50 ppm and lastly the carbons of the butyl chain (C5-C8), at 13, 17, 24 and 64 ppm. The CPMAS-NMR spectra of SSi[N<sub>3114</sub>]Cl and SSi[N<sub>3112</sub>NH<sub>2</sub>]Cl are quite similar, especially for the carbons of the free methyl chains (C4) around the cation. The main difference is regarding the influence of

the introduction of an additional amine group and the difference between the length of the alkyl chain since, in the latter, there is a decrease in the number of carbons (ethyl chain) and, consequently, the number of peaks in the spectrum (C6 and C5 at 43 and 56 ppm).

Zeta potential measurements were performed to study the surface charge of the IL-based materials. Data from the zeta potential measurements as a function of pH for the synthesized SILs are provided in the Supporting Information (Figures S1-S4). It was determined the point of zero charge (PZC), which corresponds to the pH value at which a solid particle in suspension exhibits zero net electrical charge on its surface, showing the following trend: SSi[N<sub>3112</sub>NH<sub>2</sub>]Cl < SSi[N<sub>3114</sub>]Cl < SSi[C<sub>3</sub>C<sub>1</sub>Im]Cl < SSi[C<sub>3</sub>C<sub>3</sub>NH<sub>2</sub>Im]Cl (Fig. 3). It is possible to conclude that all four synthesized SILs display higher PZC values than the starting silica (PZC of 3, value obtained from a previous work [26]), confirming the successful silica functionalization with the ILs. The presence of a



Fig. 3. Zeta potential values for each synthesized SIL.

cation in SILs confers a positively charged surface at higher pH values to these supports, influencing the PZC values. Moreover, imidazolium-based SILs present higher PZC values, meaning that for the typical working buffers (pH between 6 and 8), these supports will display a positive net charge which can enhance the interactions with the negatively charged nucleic acids.

### 3.2. Cytotoxic effect of synthesized supports

Considering the main objective of developing new chromatographic supports to be used in the purification of biomolecules with potential application as biopharmaceuticals, it is of importance to test any cytotoxic effect these ligands might present. Since sometimes ligand leaching might occur, so it is of foremost importance to guarantee the safety of the supports used in biopharmaceuticals purification. In this sense, the colorimetric assay MTT (3-(4,5-dimethylthiazol-2-yl)-2,5-diphenyltetrazolium bromide) was used for the assessment of human fibroblasts (hFIB) viability in the presence of SSi[C<sub>3</sub>C<sub>1</sub>Im]Cl, SSi[C<sub>3</sub>C<sub>3</sub>NH<sub>2</sub>Im]Cl, SSi[N<sub>3114</sub>]Cl, and SSi[N<sub>3112</sub>NH<sub>2</sub>]Cl, at three different quantities (25, 50 and 100 µg) of support. Through the analysis of Fig. 4, representing the MTT results at 24 and 48 h (A and B, respectively) of the culture of hFIB in the presence of the four SILs, it is ensured that these ligands did not induce any cytotoxic effect on these cells, except for 100 µg of SSi[N<sub>3114</sub>]Cl in which cells viability was below 80 % after 48 h, thus presenting cytotoxicity in these conditions.

It should be emphasized that ligand leaching is not expected to occur since the IL ligand is bound covalently to the support, and in the possibility of occurrence, it would not reach the amounts tested in this assay. This fact reinforces the safety of any of these supports for biopharmaceuticals purification and is in accordance with other studies regarding ILs cytotoxicity [27].

### 3.3. Screening of RNA binding/elution conditions

Aiming at characterizing the interaction profile of RNA with the prepared supports, several binding/elution studies were initially performed at different conditions. In order to study different types of interactions, we manipulated the buffer's conditions (type of buffer, salts, ionic strength, or pH) to evaluate the binding and elution capacity in each case. For example, to promote mainly electrostatic interactions for

the binding, we started with a low salt concentration in which the negatively charged nucleic acids will interact with the positively charged IL-based ligand, as the working buffer pH is established to be below the determined PZC of the IL ligand to guarantee the positive charge of the ligand and the interaction. Then, we increased salt concentration using NaCl, in which the ions will compete with the bound molecules and allow their elution. On the contrary, to promote mainly hydrophobic interactions, we started with high salt concentration, using (NH<sub>4</sub>)<sub>2</sub>SO<sub>4</sub>, in which the biomolecules establish hydrophobic interactions with the ligand. Then, by decreasing the salt concentration, the water molecules rearrange around the bound molecules, thus disfavoring the interaction and promoting elution [28]. Therefore, to evaluate the RNA binding behavior in conditions that can mainly favor electrostatic interactions, the binding step was established with 10 mM K<sub>2</sub>HPO<sub>4</sub>/KH<sub>2</sub>PO<sub>4</sub>, while the elution step was accomplished with 1.5 M NaCl in 10 mM K<sub>2</sub>HPO<sub>4</sub>/KH<sub>2</sub>PO<sub>4</sub> pH 8.0 in order to increase the ionic strength of the buffer. In this case, if the support is positively charged, the RNA could have the ability to first interact and then elute when the salt concentration increases. For the supports under evaluation and considering that at pH 8.0 they can present some positive character (except for the SSi[N<sub>3112</sub>NH<sub>2</sub>]Cl), it would be expected the RNA interaction with the SILs. The RNA binding and elution results were analyzed by absorbance measurement at 260 nm (data not shown), calculating then the percentage of unbound or eluted RNA in each chromatographic step. Thus, the performance of all prepared SILs to retain/elute a recombinant small RNA sample was addressed, whose results are presented in Fig. 5.

For all the functionalized supports, most of RNA is retained and it is only eluted by increasing the ionic strength. With SSi[C<sub>3</sub>C<sub>3</sub>NH<sub>2</sub>Im]Cl, SSi[N<sub>3114</sub>]Cl, and SSi[N<sub>3112</sub>NH<sub>2</sub>]Cl, the RNA sample was totally bound to the column, eluting around 68% to 100% of the RNA with the increased salt concentration. With SSi[C<sub>3</sub>C<sub>1</sub>Im]Cl the interaction was not total, but all bound RNA was recovered with 1.5 M of NaCl. Such interactions are expected given the IL chemical structure, especially regarding its positively charged amine group. Additionally, by the PZC results depicted in Fig. 3, it is inferred that for pH 8.0, the condition established for the RNA binding, the SSi[C<sub>3</sub>C<sub>3</sub>NH<sub>2</sub>Im]Cl support presents more positive charges at the surface than the SSi[C<sub>3</sub>C<sub>1</sub>Im]Cl. In accordance, this support (SSi[C<sub>3</sub>C<sub>3</sub>NH<sub>2</sub>Im]Cl) promoted a stronger RNA binding, resulting in a decreased recovery, being required higher concentrations of NaCl to

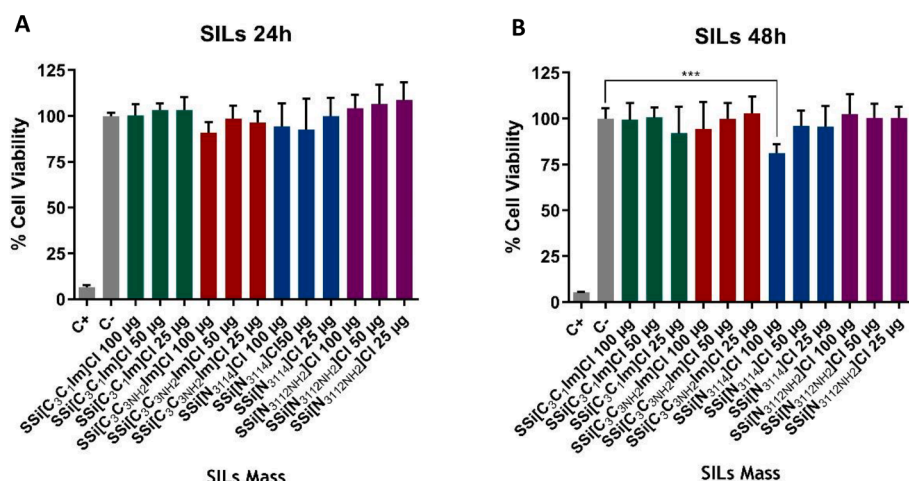


Fig. 4. Cellular viability (MTT assay) of human fibroblasts after 24 h (A) and 48 h (B) incubation with the different supports. Untreated cells (C<sup>+</sup>) and ethanol treated cells (C<sup>-</sup>) were used as negative and positive control, respectively. Viability percentage is expressed relatively to the control cells. Values were calculated with the data obtained from three independent measurements (mean ± SD, n = 3). Statistical analysis was performed using "One-way ANOVA". (ns = p > 0.05; \*\*\* p ≤ 0.001).

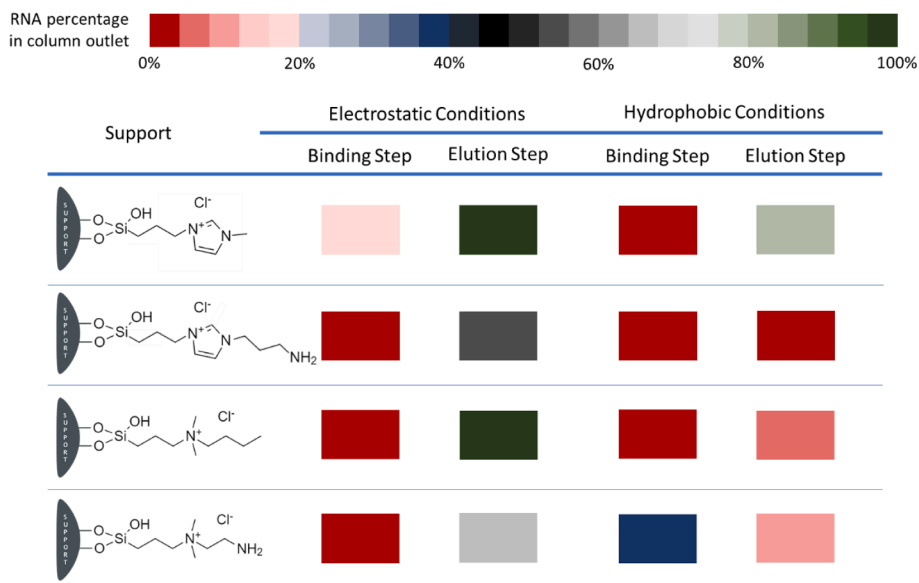


Fig. 5. Schematic representation of the binding and elution assays performed with the synthesized supports.

elute all the bound RNA (data not shown) comparatively to the SSI [C<sub>3</sub>C<sub>1</sub>Im]Cl. However, regarding the global results for the supports not possessing the imidazolium group, this was not verified, meaning that additional interactions can occur between RNA and these ligands.

To demonstrate if these IL-based ligands behave as multimodal moieties, the RNA binding behavior was studied under conditions that mainly favor hydrophobic interactions, to investigate further which non-covalent interactions are mainly responsible for the RNA retention onto these supports. For this, the RNA binding step was defined as 2 M (NH<sub>4</sub>)<sub>2</sub>SO<sub>4</sub> in 10 mM K<sub>2</sub>HPO<sub>4</sub>/KH<sub>2</sub>PO<sub>4</sub> pH 8.0, while the elution step was accomplished with 10 mM K<sub>2</sub>HPO<sub>4</sub>/KH<sub>2</sub>PO<sub>4</sub> pH 8.0 in order to decrease the ionic strength of the buffer. When these conditions were favored, the supports SSI[C<sub>3</sub>C<sub>1</sub>Im]Cl, SSI[C<sub>3</sub>C<sub>3</sub>NH<sub>2</sub>Im]Cl, SSI[N<sub>3114</sub>]Cl, showed higher ability for RNA binding, contrary to what was observed with SSI[N<sub>3112</sub>NH<sub>2</sub>]Cl that only retained half of the injected RNA. Moreover, in the supports SSI[C<sub>3</sub>C<sub>3</sub>NH<sub>2</sub>Im]Cl, SSI[N<sub>3114</sub>]Cl, and SSI[N<sub>3112</sub>NH<sub>2</sub>]Cl, it was verified that the bound RNA did not elute by decreasing the ammonium sulphate concentration. In contrast, with SSI[C<sub>3</sub>C<sub>1</sub>Im]Cl almost all bound RNA was recovered in these conditions. Since the decrease in the ionic strength to 10 mM K<sub>2</sub>HPO<sub>4</sub>/KH<sub>2</sub>PO<sub>4</sub> (pH 8) was not an efficient condition for the RNA recovery from the majority of the SILs in study, this might suggest that other interactions rather than hydrophobic interactions are involved, as it was foreseen before. The elution with the K<sub>2</sub>HPO<sub>4</sub>/KH<sub>2</sub>PO<sub>4</sub> buffer (pH 8) was intended to minimize the hydrophobic interactions established, but at the same time, this condition can favor the electrostatic interactions, thus not being enough for the recovery of loaded RNA. Actually, in the previous experiments performed with conditions promoting electrostatic interactions, RNA binding was achieved when using K<sub>2</sub>HPO<sub>4</sub>/KH<sub>2</sub>PO<sub>4</sub> buffer, supporting this result. To further explore the possibility of recovering the bound RNA, a second elution step was included in the gradient, using 1.5 M NaCl in 10 mM K<sub>2</sub>HPO<sub>4</sub>/KH<sub>2</sub>PO<sub>4</sub>, pH 8. In this step, it was verified the effective elution of the majority of bound RNA. This chromatographic behavior, where different interactions, namely hydrophobic and electrostatic interactions, occur between the RNA and the prepared SILs, is often associated with ligands possessing a multimodal character. This is characterized by more than one form of non-covalent chemical interaction occurring between the specific ligands immobilized onto the stationary phase and the target molecules [29]. According to the chemical structure of SSI[C<sub>3</sub>C<sub>1</sub>Im]Cl, which possesses both an imidazolium functional group and a positively charged cation, it would be expected the establishment of both hydrophobic and electrostatic

interactions (among others) with RNA. Moreover, the SSI[C<sub>3</sub>C<sub>3</sub>NH<sub>2</sub>Im]Cl, which differs from the previous SIL by the introduction of an amine group in the imidazolium, is prone to present a more hydrophobic and electrostatic feature, being the interaction with RNA stronger than with the original SSI[C<sub>3</sub>C<sub>1</sub>Im]Cl, in both conditions. With this specific chromatographic support, when favoring hydrophobic interactions, the binding was so effective that decreasing or removing the (NH<sub>4</sub>)<sub>2</sub>SO<sub>4</sub> from the buffer was not enough to promote the elution of RNA, and actually the RNA % in column outlet was extremely low. By using the (NH<sub>4</sub>)<sub>2</sub>SO<sub>4</sub> in the binding buffer, RNA interacts with the ligands mainly by hydrophobic interactions. However, when removing this salt from the buffer other type of interactions are established preventing the RNA elution. After the binding step with 1.5 M of (NH<sub>4</sub>)<sub>2</sub>SO<sub>4</sub>, we tested 2 M of NaCl for the elution and the recovery increased to 15% (data not shown). For this reason, the recovery was only possible when increasing the NaCl concentration. This is an interesting result that also proves the multimodal behavior of this support.

Regarding the SSI[N<sub>3114</sub>]Cl, it also proved its multimodal capacity, due to the good binding properties when both electrostatic and hydrophobic interactions were favored. This ligand, at pH 8, presents a positive charge pivotal for the interaction established with the negatively charged RNA, when electrostatic interactions were favored. Additionally, when analyzing the hydrophobic interactions promoted by the SSI[N<sub>3114</sub>]Cl support, it is possible to conclude that the main contribution is from the alkyl chains. In regard to the SSI[N<sub>3112</sub>NH<sub>2</sub>]Cl, where an amine group was added to the last SIL and the alkyl chain was shortened, it can be concluded that both hydrophobic and electrostatic interactions were highly affected since not only the surface charge of this SIL was decreased but also the interaction with RNA under hydrophobic conditions was unfavorable.

Overall, by using the prepared supports to interact with RNA, it was found a multimodal behavior for most of the ligands (SSI[C<sub>3</sub>C<sub>1</sub>Im]Cl, SSI[C<sub>3</sub>C<sub>3</sub>NH<sub>2</sub>Im]Cl, and SSI[N<sub>3114</sub>]Cl), what can be highly desirable to find selectivity and achieve an effective separation of nucleic acids. The main advantage is the possibility of exploiting different interactions and distinguishing between nucleic acid species. Moreover, the binding pattern in both ionic and hydrophobic conditions may allow the selection of milder binding/elution buffers, which brings additional benefits for the process and the isolated products, with positive environmental impact (for example, by using sodium chloride instead of ammonium sulfate). Accordingly, the purification performance of the nucleic acids was further evaluated under conditions that favor electrostatic interactions.

Besides, based on these initial screening assays,  $\text{SSi}[\text{C}_3\text{C}_1\text{Im}]\text{Cl}$ ,  $\text{SSi}[\text{C}_3\text{C}_3\text{NH}_2\text{Im}]\text{Cl}$ , and  $\text{SSi}[\text{N}_{3114}]\text{Cl}$  seemed to be the most promising supports for further purification assays. Since  $\text{SSi}[\text{N}_{3114}]\text{Cl}$  demonstrated some cytotoxicity and  $\text{SSi}[\text{C}_3\text{C}_1\text{Im}]\text{Cl}$  has already been tested by the group and proven to show good selectivity between gDNA and RNA [4], the  $\text{SSi}[\text{C}_3\text{C}_3\text{NH}_2\text{Im}]\text{Cl}$  was identified as the most relevant support to be further explored. This support was then applied in the selective separation of nucleic acids (gDNA and RNA) from complex bacterial mixtures, and the results were analyzed in terms of selectivity and reproducibility.

### 3.4. Separation between nucleic acids

After the screening assays, the  $\text{SSi}[\text{C}_3\text{C}_3\text{NH}_2\text{Im}]\text{Cl}$  was packed in a chromatographic column (GE Healthcare, Uppsala, Sweden), and the experiments were conducted in an AKTA Avant® system under the control of Unicorn 6 software (GE Healthcare, Uppsala, Sweden) at room temperature (ca. 25 °C).

The retention profile of RNA was initially investigated, by performing a chromatographic assay, in the conditions previously established (Figs. 6 and 7, Assay 1 - Pink). All the RNA sample interacted with the ligand, being eluted only with the increase in salt concentration to 1.5 M of NaCl, which was in accordance with the previous screening assays. After this, it was intended to study the chromatographic profile of DNA to evaluate its interaction behavior with the  $\text{SSi}[\text{C}_3\text{C}_3\text{NH}_2\text{Im}]\text{Cl}$  support and infer the possible selectivity towards RNA. An *E. coli* DH5 $\alpha$  lysate sample, initially composed of genomic DNA (gDNA) and RNA, was treated with RNase to evaluate the chromatographic profile of gDNA (Figs. 6 and 7, Assay 2 - Purple). The injection of this gDNA-containing sample, using the same gradient, resulted in a chromatogram showing a peak in the flowthrough; however, it was not possible to visualize any band corresponding to the gDNA upon analyzing the respective chromatographic fractions in the agarose gel electrophoresis (Fig. 7, FT). Thus, it was concluded that this peak did not correspond to any nucleic acid form. In the elution step, with 1.5 M of NaCl, a small peak was obtained that corresponded to the residual RNA of the initial lysate sample, which was not completely digested by RNase (Fig. 7, P). Still,

gDNA was not observed in the agarose gel, meaning that it was strongly bound to this ligand and was not eluted during the chromatographic assay. In order to understand the chromatographic profile and identify the species eluting in the flowthrough (first peak), additional experiments were performed. Considering that the initial sample was a complex lysate, other contaminating biomolecules could be present in the sample. Thus, a protein quantification assay was carried out through the Bradford method, but the results did not reveal the presence of proteins in these fractions (data not shown). Afterward, the UV spectra of this peak revealed a maximum absorbance at 230 nm. With this result, it is suggested that other impurities from the lysate sample were eluting at the binding step conditions, such as organic solvents used during the extraction procedure (guanidinium thiocyanate) that were not completely removed.

To further confirm the capacity of the  $\text{SSi}[\text{C}_3\text{C}_3\text{NH}_2\text{Im}]\text{Cl}$  support to separate gDNA and RNA from complex samples, a lysate sample was directly loaded onto the column (Figs. 6 and 7, Assay 3 - Red). The chromatographic profile was similar to the one obtained in the previous assay, with a first peak appearing in the flowthrough and the elution of RNA with higher salt concentration. Also, in this case, the elution of gDNA was not verified in none of the peaks (confirmed by the absence of the corresponding band in the electrophoresis), proving the strong interaction of this biomolecule with the support. The performance of the support to isolate RNA was also analyzed in more complex samples. For this, it was loaded onto the  $\text{SSi}[\text{C}_3\text{C}_3\text{NH}_2\text{Im}]\text{Cl}$ , a sample containing gDNA, supercoiled plasmid DNA (sc pDNA), open circular pDNA (oc pDNA), and RNA (Figs. 6 and 7, Assay 4 - Green). The results revealed that all DNA species present a strong interaction with the IL-based ligand, being totally retained in the column.

These results are of interest when compared to the previous work of our research group [4], in which the support MP-SilPrMimCl (macroporous support with the 1-methyl-3-propylimidazolium chloride IL as ligand) successfully separated RNA from DNA. In that work, the retention profile of nucleic acids was similar to the one observed in the present study, meaning that RNA eluted first and DNA eluted lastly by increasing the salt concentration. The main difference between the previous MP-SilPrMimCl and the novel  $\text{SSi}[\text{C}_3\text{C}_3\text{NH}_2\text{Im}]\text{Cl}$  support

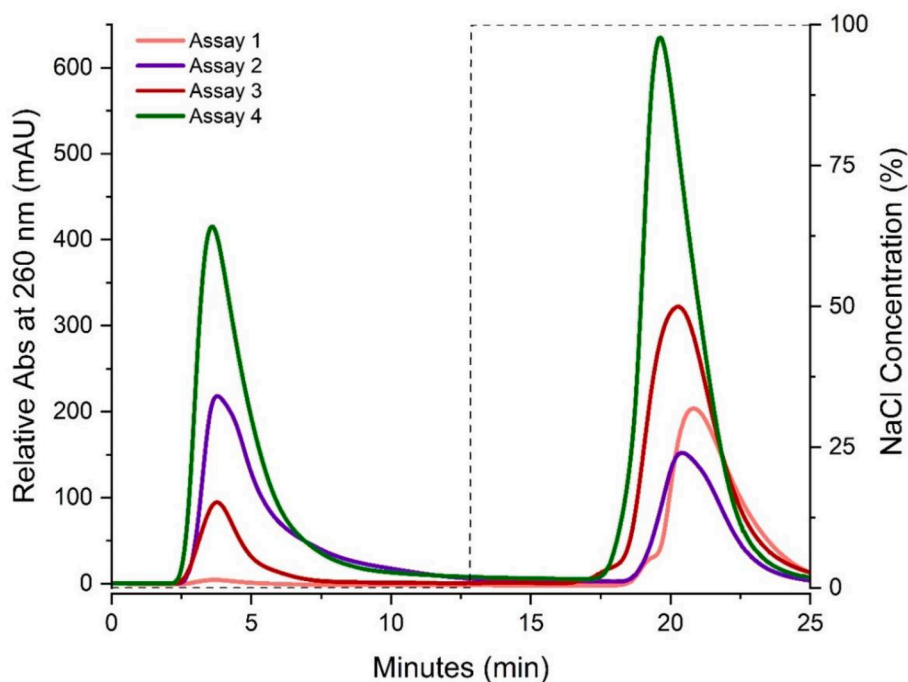


Fig. 6. Representative chromatograms of the assays performed in  $\text{SSi}[\text{C}_3\text{C}_3\text{NH}_2\text{Im}]\text{Cl}$ . The binding was favored with low salt concentration followed by a stepwise gradient and a washing step (not shown).



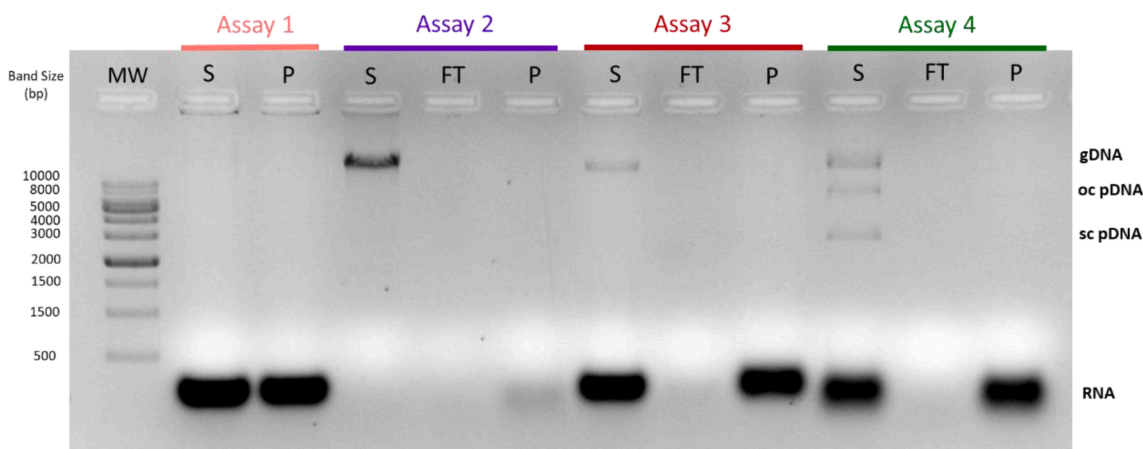


Fig. 7. Agarose gel electrophoresis of the fractions recovered from the assays represented in Fig. 6. S-Sample, P-Peak, FT-Flowthrough.

studied here the presence of an amine group bound to the imidazolium ring through an alkyl propyl chain. This functional group is responsible for an even stronger interaction with DNA, resulting from both hydrogen bonding and electrostatic interactions [30]. This interaction mechanism justifies the higher interaction between this support and DNA, comparatively to what was observed with MP-SilPrMImCl, in which increased salt concentration was enough to elute the bound DNA. Given the similar structure between MP-SilPrMImCl and the SSI[C<sub>3</sub>C<sub>3</sub>NH<sub>2</sub>Im]Cl, it would be expected that the support tested in this work could also be applied to more complex samples.

It should be noted that in studied lysate extractions, there were not used hazardous and toxic organic solvents like phenol and chloroform, which are usually used for standard RNA extraction protocols [31]. By purifying these more complex samples with a simple, rapid and robust chromatographic procedure, it is possible to effectively separate RNA from gDNA and eliminate organic compounds that were present in the initial sample and could eventually compromise RNAs stability.

### 3.5. Molecular docking analysis

The initial screening revealed the influence of the solvent on the interaction between silica-based supports and nucleic acids. However, to

understand the differential affinity of DNA and RNA towards SSI [C<sub>3</sub>C<sub>3</sub>NH<sub>2</sub>Im]Cl observed experimentally, it is crucial to analyze the specific interactions responsible for nucleic acid selective separation. Therefore, molecular docking analysis was employed to identify the binding interactions of both complexes (SSI[C<sub>3</sub>C<sub>3</sub>NH<sub>2</sub>Im]Cl-DNA and SSI [C<sub>3</sub>C<sub>3</sub>NH<sub>2</sub>Im]Cl-RNA). The intermolecular interactions between SSI [C<sub>3</sub>C<sub>3</sub>NH<sub>2</sub>Im]Cl and DNA/RNA were predicted using molecular docking. The docking scores, types of interaction, and geometry distances (Å) of the SSI[C<sub>3</sub>C<sub>3</sub>NH<sub>2</sub>Im]Cl-DNA/RNA complexes are reported in the Supporting Information (Table S1). Fig. 8 shows the binding pose of SSI [C<sub>3</sub>C<sub>3</sub>NH<sub>2</sub>Im]Cl with the lowest docking score on the DNA/RNA surface. The results demonstrate that SSI[C<sub>3</sub>C<sub>3</sub>NH<sub>2</sub>Im]Cl bind with higher docking score with DNA (-7.1 kcal.mol<sup>-1</sup>) in comparison with RNA (-6.6 kcal.mol<sup>-1</sup>), and hydrogen bond interactions were the only interactions observed in both complexes. However, the SSI[C<sub>3</sub>C<sub>3</sub>NH<sub>2</sub>Im]Cl-DNA complex displays a higher hydrogen bond ability compared to SSI [C<sub>3</sub>C<sub>3</sub>NH<sub>2</sub>Im]Cl-RNA. Moreover, SSI[C<sub>3</sub>C<sub>3</sub>NH<sub>2</sub>Im]Cl-DNA interactions occurred with Thymidine, Guanosine, and Adenosine, while SSI [C<sub>3</sub>C<sub>3</sub>NH<sub>2</sub>Im]Cl-RNA interactions were observed with Guanosine and Adenosine (Fig. 8). The interactions from SSI[C<sub>3</sub>C<sub>3</sub>NH<sub>2</sub>Im]Cl to DNA (6 interactions) come from the ligand alkyl chain, aromatic ring, amine and hydroxyl group to oxygens of DNA. On the other hand, 4 non-covalent

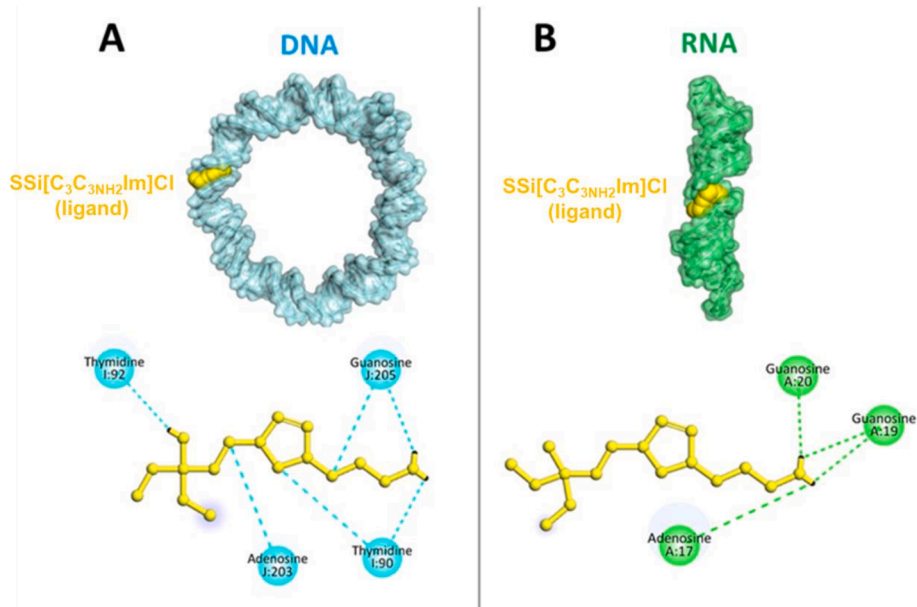


Fig. 8. Docking pose with the lowest score (kcal.mol<sup>-1</sup>) and 2D interaction diagram for: (A) SSI[C<sub>3</sub>C<sub>3</sub>NH<sub>2</sub>Im]Cl -DNA and (B) SSI[C<sub>3</sub>C<sub>3</sub>NH<sub>2</sub>Im]Cl -RNA complexes.

bonds from  $\text{SSi}[\text{C}_3\text{C}_3\text{NH}_2\text{Im}]\text{Cl}$  were identified, all from the ligand amine group to RNA. The molecular docking analysis of ILs with nucleic acids were previously reported by Singh and co-workers [32], showing that all ILs studied display high ability to promote hydrogen bonding with nucleic acids. The authors have concluded that the primary driving force behind the stabilization of the IL-DNA complex is due to polar interactions, specifically hydrogen bonding. Thus, the hydrogen bond ability of  $\text{SSi}[\text{C}_3\text{C}_3\text{NH}_2\text{Im}]\text{Cl}$  with nucleic acids seems to be the major driving force behind the selective behavior in separating DNA and RNA. Additionally, it should be noted that hydrophobic and electrostatic interactions may also occur simultaneously on the structure of DNA/RNA due to the solvent used as an elution buffer.

### 3.6. Circular Dichroism analysis of RNA

In order to evaluate the integrity and stability of RNA samples after the purification assays, CD spectra were obtained for the RNA purified with the  $\text{SSi}[\text{C}_3\text{C}_3\text{NH}_2\text{Im}]\text{Cl}$  support. Typical RNA CD spectra are characterized by having two main ellipticity peaks: a maximum at approximately 265 nm (positive band) and a minimum at approximately 210 nm (negative band) [33]. In Fig. 9, the RNA spectrum is represented in purple line, and it is possible to verify the two characteristic bands at 265 and 210 nm. The RNA spectrum from a purified fraction obtained with  $\text{SSi}[\text{C}_3\text{C}_3\text{NH}_2\text{Im}]\text{Cl}$  is represented in red line, in which it is possible to observe the CD profile's maintenance, demonstrating that RNA structure is maintained after purification.

## 4. Conclusion

This work described the functionalization of commercial silica with four ILs acting as multimodal ligands to prepare innovative chromatographic supports. After synthesizing and characterizing the materials, their ability to interact and separate different nucleic acids was studied in preparative liquid chromatography. In particular, four SILs ( $\text{SSi}[\text{C}_3\text{C}_1\text{Im}]\text{Cl}$ ,  $\text{SSi}[\text{C}_3\text{C}_3\text{NH}_2\text{Im}]\text{Cl}$ ,  $\text{SSi}[\text{N}_{3114}]\text{Cl}$ , and  $\text{SSi}[\text{N}_{3112\text{NH}_2}]\text{Cl}$ ) were synthesized and characterized by elemental analysis, CPMAS-NMR and Point Zero Charge (PZC). All the prepared materials were successfully functionalized, and their surface was positively charged at pH 7, being the  $\text{SSi}[\text{C}_3\text{C}_3\text{NH}_2\text{Im}]\text{Cl}$ , the support with a higher PZC value. Concerning the cytotoxicity assays performed with these prepared SILs, it was possible to ascertain that these ligands did not induce any cytotoxic effect on human fibroblasts cells, except for the use of 100  $\mu\text{g}$  of  $\text{SSi}[\text{N}_{3114}]\text{Cl}$ , in which cells viability was below 80 %. Despite this fact, this would not be a concern since leaching of the ligand is not expected to

occur during the purification assays, much less in these tested concentrations.

With the initial screening of binding and elution of RNA samples for each synthesized support, it was possible to verify the multimodal behavior in 3 of the 4 ligands, since they could establish multiple interactions with RNA, when electrostatic or hydrophobic conditions were used. After this screening, the  $\text{SSi}[\text{C}_3\text{C}_3\text{NH}_2\text{Im}]\text{Cl}$  was chosen for further RNA purification, as this support showed to be the most promising not only for RNA binding but also considering the recovery and the possibility to exploit RNA interaction in milder conditions. This support was then applied in the selective separation of nucleic acids (DNA and RNA) from complex bacterial mixtures, leading to noteworthy results regarding selectivity and reproducibility. Furthermore, the RNA purified with this multimodal ligand attained a significant purity level, without detecting residual proteins and organic compounds. Furthermore, high integrity of RNA was achieved, as ascertained by CD spectroscopy.

The most interesting fact achieved with the  $\text{SSi}[\text{C}_3\text{C}_3\text{NH}_2\text{Im}]\text{Cl}$  support was that upon the loading of different mixtures of DNA and RNA, using gradient conditions that could favor electrostatic interactions, it was verified that all DNA species remained strongly bound onto the column and were not eluted. Bound DNA was most likely removed during the regeneration since the reported results were very reproducible for at least 5 chromatographic cycles before proceeding to the regeneration. Interestingly, this support can be easily regenerated with NaOH and HCl aqueous solutions to be reused, being highly reproducible and without compromising its separation performance. By using this chromatographic ligand, other impurities that are still present in lysate samples, such as organic solvents used in the extraction procedure (guanidinium thiocyanate), could be eluted separately from the RNA. Therefore, the designed purification technique is highly promising for the purification of RNA samples. Overall, the obtained results contribute towards designing more sustainable purification techniques of nucleic acids, avoiding the use of hazardous extraction solvents. Since the  $\text{SSi}[\text{C}_3\text{C}_3\text{NH}_2\text{Im}]\text{Cl}$  acts as a multimodal ligand, this type of chromatographic support deserves to be investigated for the purification of different RNA species (coding or non-coding RNAs), with potential use as biopharmaceuticals. Besides, it would be interesting also to consider this support as a potential substitution of the standard RNA extraction/purification protocols and consequently eliminate phenol/chloroform usage. Additionally, it would definitely be of interest the study of these resins for purification of PCR products since an efficient separation was observed between larger (gDNA and pDNA) molecules that were retained in the column and much smaller molecules (low molecular weight RNA). Considering the simple and straightforward conditions used for the RNA separation, this protocol could easily be performed in bench columns and thus contribute to implementing greener processes for RNA preparation.

### CRediT authorship contribution statement

**Rita Carapito:** Conceptualization, Methodology, Investigation, Validation, Writing – original draft. **Sandra C. Bernardo:** Conceptualization, Methodology, Investigation, Validation, Writing – original draft. **Matheus M. Pereira:** Conceptualization, Methodology, Investigation, Validation, Writing – original draft. **Márcia C. Neves:** Conceptualization, Methodology, Investigation, Validation, Writing – original draft. **Mara G. Freire:** Conceptualization, Methodology, Resources, Writing – review & editing, Supervision, Project administration, Funding acquisition. **Fani Sousa:** Conceptualization, Methodology, Resources, Writing – review & editing, Supervision, Project administration, Funding acquisition.

### Declaration of Competing Interest

The authors declare the following financial interests/personal relationships which may be considered as potential competing interests:

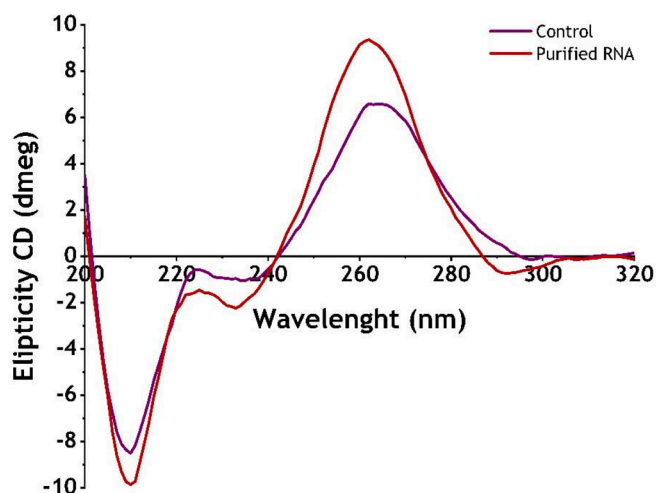


Fig. 9. CD spectra (200 – 320 nm) of RNA collected from the purification assays with  $\text{SSi}[\text{C}_3\text{C}_3\text{NH}_2\text{Im}]\text{Cl}$ .

[Rita Carapito reports financial support was provided by Foundation for Science and Technology. Marcia C. Neves reports financial support was provided by Foundation for Science and Technology. Fani Sousa reports financial support was provided by European Commission. Mara G. Freire reports financial support was provided by European Commission. Mara G. Freire and Fani Sousa has patent pending to Universidade de Aveiro and University of Beira Interior. Mara G. Freire is a member of the Editorial Board of Separation and Purification Technology.].

## Data availability

Data will be made available on request.

## Acknowledgements

The authors acknowledge the funding from Portuguese Foundation for Science and Technology (FCT), through the projects UIDB/00709/2020, UIDP/00709/2020 and the project PTDC/BII-BBF/29496/2017 funded by FEDER, through COMPETE2020-POCI, and by national funds, through FCT/MCTES. This work was also developed within the scope of the project CICECO-Aveiro Institute of Materials, UIDB/50011/2020, UIDP/50011/2020 & LA/P/0006/2020, financed by national funds through the FCT/MCTES (PIDDAC). CIEPQPF is supported by the FCT through the projects UIDB/EQU/00102/2020 and UIDP/EQU/00102/2020. The work was developed within the scope of the EIC-Pathfinder YSCRIPT project with reference 101047. The NMR spectrometers are part of the National NMR Network (PTNMR) and are partially supported by Infrastructure Project N<sup>o</sup> 022161 (co-financed by FEDER through COMPETE 2020, POCI and PORK and FCT through PIDDAC). Rita Carapito and Márcia C. Neves acknowledge FCT for the PhD fellowship (2020.07980.BD) and the research contract CEECIND/00383/2017, respectively.

## Appendix A. Supplementary material

Supplementary data to this article can be found online at <https://doi.org/10.1016/j.seppur.2023.123676>.

## References

- [1] A.B. Hill, M. Chen, C.-K. Chen, B.A. Pfeifer, C.H. Jones, Overcoming Gene-Delivery Hurdles: Physiological Considerations for Nonviral Vectors, *Trends Biotechnol.* 34 (2) (2016) 91–105.
- [2] J.F.A. Valente, J.A. Queiroz, F. Sousa, Dilemma on plasmid DNA purification: binding capacity vs selectivity, *J. Chromatogr. A* 1637 (2021), 461848.
- [3] L. Baronti, H. Karlsson, M. Marušič, K. Petzold, A guide to large-scale RNA sample preparation, *Anal. Bioanal. Chem.* 410 (14) (2018) 3239–3252.
- [4] M.C. Neves, P. Pereira, A.Q. Pedro, J.C. Martins, T. Trindade, J.A. Queiroz, M. G. Freire, F. Sousa, Improved ionic-liquid-functionalized macroporous supports able to purify nucleic acids in one step, *Materials Today Bio* 8 (2020), 100086.
- [5] B. Baptista, M. Riscado, J.A. Queiroz, C. Pichon, F. Sousa, Non-coding RNAs: Emerging from the discovery to therapeutic applications, *Biochem. Pharmacol.* 189 (2021), 114469.
- [6] S. Fekete, C. Doneanu, B. Addepalli, M. Gaye, J. Nguyen, B. Alden, R. Birdsall, D. Han, G. Isaac, M. Lauber, Challenges and emerging trends in liquid chromatography-based analyses of mRNA pharmaceuticals, *J. Pharm. Biomed. Anal.* 224 (2023), 115174.
- [7] P. Pereira, A.Q. Pedro, J.A. Queiroz, A.R. Figueiras, F. Sousa, New insights for therapeutic recombinant human miRNAs heterologous production: *Rhodovulum sulfidophilum* vs *Escherichia coli*, *Bioengineered* 8 (5) (2017) 670–677.
- [8] S.C. Tan, B.C. Yip, DNA, RNA, and Protein Extraction: The Past and The Present, *J. Biomed. Biotechnol.* 2009 (2009), 574398.
- [9] A. Azarani, K.H. Hecker, RNA analysis by ion-pair reversed-phase high performance liquid chromatography, *Nucleic Acids Res.* 29 (2) (2001) e7–e.
- [10] P. Li, M. Li, F. Zhang, M. Wu, X. Jiang, B. Ye, Z. Zhao, D. Yue, Q. Fan, H. Chen, High-efficient nucleic acid separation from animal tissue samples via surface modified magnetic nanoparticles, *Sep. Purif. Technol.* 262 (2021), 118348.
- [11] S.P.M. Ventura, F.A. e Silva, M.V. Quental, D. Mondal, M.G. Freire, J.A. P. Coutinho, Ionic-Liquid-Mediated Extraction and Separation Processes for Bioactive Compounds: Past, Present, and Future Trends, *Chem. Rev.* 117 (10) (2017) 6984–7052.
- [12] M.G. Freire, A.F.M. Cláudio, J.M.M. Araújo, J.A.P. Coutinho, I.M. Marrucho, J.N. C. Lopes, L.P.N. Rebelo, Aqueous biphasic systems: a boost brought about by using ionic liquids, *Chem. Soc. Rev.* 41 (14) (2012) 4966–4995.
- [13] S. Fister, S. Fuchs, P. Mester, I. Kilpeläinen, M. Wagner, P. Rossmanith, The use of ionic liquids for cracking viruses for isolation of nucleic acids, *Sep. Purif. Technol.* 155 (2015) 38–44.
- [14] T.E. Sintra, M. Nasirpour, F. Siopa, A.A. Rosatella, F. Gonçalves, J.A.P. Coutinho, C. A.M. Afonso, S.P.M. Ventura, Ecotoxicological evaluation of magnetic ionic liquids, *Ecotoxicol. Environ. Saf.* 143 (2017) 315–321.
- [15] B. Kudlak, K. Owczarek, J. Namieśnik, Selected issues related to the toxicity of ionic liquids and deep eutectic solvents—a review, *Environ. Sci. Pollut. Res.* 22 (16) (2015) 11975–11992.
- [16] Q. Wang, G.A. Baker, S.N. Baker, L.A. Colón, Surface confined ionic liquid as a stationary phase for HPLC, *Analyst* 131 (9) (2006) 1000–1005.
- [17] W.-Z. Zhang, L.-J. He, X. Liu, S.-X. Jiang, Ionic liquids as mobile phase additives for separation of nucleotides in high-performance liquid chromatography, *Chin. J. Chem.* 22 (6) (2004) 549–552.
- [18] S.C. Bernardo, R. Carapito, M.C. Neves, M.G. Freire, F. Sousa, Supported Ionic Liquids Used as Chromatographic Matrices in Bioseparation—An Overview, *Molecules* 27 (5) (2022) 1618.
- [19] P. Pereira, A. Sousa, J. Queiroz, I. Correia, A. Figueiras, F. Sousa, Purification of pre-miR-29 by arginine-affinity chromatography, *J. Chromatogr. B* 951–952 (2014) 16–23.
- [20] R. Martins, J.A. Queiroz, F. Sousa, Histidine affinity chromatography-based methodology for the simultaneous isolation of *Escherichia coli* small and ribosomal RNA, *Biomed. Chromatogr.* 26 (7) (2012) 781–788.
- [21] H. Qiu, S. Jiang, X. Liu, N-Methylimidazolium anion-exchange stationary phase for high-performance liquid chromatography, *J. Chromatogr. A* 1103 (2) (2006) 265–270.
- [22] P. Pereira, A.Q. Pedro, M.C. Neves, J.C. Martins, I. Rodrigues, M.G. Freire, F. Sousa, Efficient Isolation of Bacterial RNAs Using Silica-Based Materials Modified with Ionic Liquids, *Life* 11 (10) (2021) 1090.
- [23] J.C.F. Nunes, M.R. Almeida, R.M.F. Bento, M.M. Pereira, V.C. Santos-Ebinuma, M. C. Neves, M.G. Freire, A.P.M. Tavares, Enhanced Enzyme Reuse through the Bioconjugation of L-Asparaginase and Silica-Based Supported Ionic Liquid-like Phase Materials, *Molecules* 27 (3) (2022) 929.
- [24] O. Trott, A.J. Olson, AutoDock Vina: Improving the speed and accuracy of docking with a new scoring function, efficient optimization, and multithreading, *J. Comput. Chem.* 31 (2) (2010) 455–461.
- [25] G.M. Morris, R. Huey, W. Lindstrom, M.F. Sanner, R.K. Belew, D.S. Goodsell, A. J. Olson, AutoDock4 and AutoDockTools4: Automated docking with selective receptor flexibility, *J. Comput. Chem.* 30 (16) (2009) 2785–2791.
- [26] S.C. Bernardo, B.R. Araújo, A.C.A. Sousa, R.A. Barros, A.C. Cristovão, M.C. Neves, M.G. Freire, Supported Ionic Liquids for the Efficient Removal of Acetylsalicylic Acid from Aqueous Solutions, *Eur. J. Inorg. Chem.* 2020 (24) (2020) 2380–2389.
- [27] S. Stolte, J. Arning, U. Bottin-Weber, A. Müller, W.-R. Pitner, U. Welz-Biermann, B. Jastorff, J. Ranke, Effects of different head groups and functionalised side chains on the cytotoxicity of ionic liquids, *Green Chem.* 9 (7) (2007) 760–767.
- [28] F. Sousa, D.M.F. Prazeres, J.A. Queiroz, Affinity chromatography approaches to overcome the challenges of purifying plasmid DNA, *Trends Biotechnol.* 26 (9) (2008) 518–525.
- [29] T. Matos, J.A. Queiroz, L. Bülow, Plasmid DNA purification using a multimodal chromatography resin, *J. Mol. Recognit.* 27 (4) (2014) 184–189.
- [30] W. Sheng, W. Wei, J. Li, X. Qi, G. Zuo, Q. Chen, X. Pan, W. Dong, Amine-functionalized magnetic mesoporous silica nanoparticles for DNA separation, *Appl. Surf. Sci.* 387 (2016) 1116–1124.
- [31] P. Chomczynski, N. Sacchi, The single-step method of RNA isolation by acid guanidinium thiocyanate–phenol–chloroform extraction: twenty-something years on, *Nat. Protoc.* 1 (2) (2006) 581–585.
- [32] N. Singh, M. Sharma, D. Mondal, M.M. Pereira, K. Prasad, Very High Concentration Solubility and Long-Term Stability of DNA in an Ammonium-Based Ionic Liquid: A Suitable Medium for Nucleic Acid Packaging and Preservation, *ACS Sustain. Chem. Eng.* 5 (2) (2017) 1998–2005.
- [33] H. Yao, E. Wynendaele, X. Xu, A. Kosgei, B. De Spiegeleer, Circular dichroism in functional quality evaluation of medicines, *J. Pharm. Biomed. Anal.* 147 (2018) 50–64.